The $(g-2)_\mu$ in the standard model: status and perspectives

Gilberto Colangelo

UNIVERSITÄT BERN

AEC
ALBERT EINSTEIN CENTER
FOR FUNDAMENTAL PHYSICS

"The $(g-2)_\mu$ puzzle", Bologna, November 15, 2023

Outline

Introduction: $(g-2)_\mu$ in the Standard Model

Hadronic light-by-light

Hadronic Vacuum Polarization contribution
- Data-driven approach
- Lattice vs data-driven: intermediate window
- The MUonE experiment
- Radiative corrections with a dispersive approach: A_{FB} and σ

Conclusions and Outlook

Outline

Introduction: $(g-2)_\mu$ in the Standard Model

Hadronic light-by-light

Hadronic Vacuum Polarization contribution
- Data-driven approach
- Lattice vs data-driven: intermediate window
- The MUonE experiment
- Radiative corrections with a dispersive approach: A_{FB} and σ

Conclusions and Outlook

History of a_μ measurements

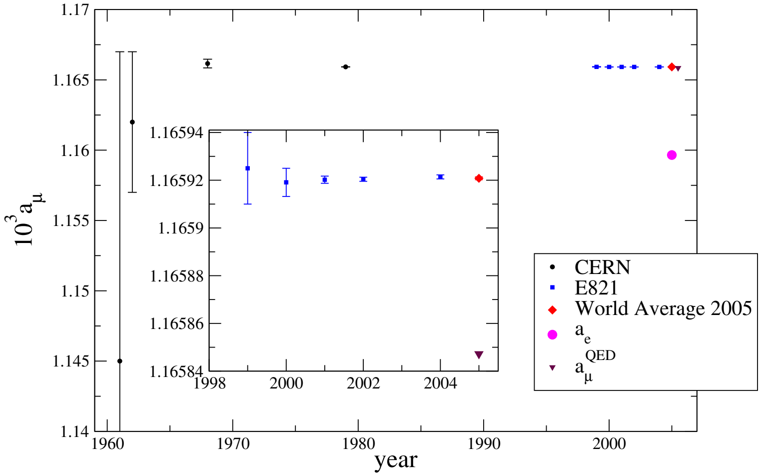

a_μ, QED and the SM

World Average (before FNAL)

$$a_\mu^{\mathrm{exp}} = (116\,592\,089 \pm 63) \times 10^{-11}$$

a_μ, QED and the SM

World Average (before FNAL)

$$a_\mu^{\mathrm{exp}} = (116\,592\,089 \pm 63) \times 10^{-11}$$

- The bulk of the difference between a_e and a_μ is due to QED and originates from large logs of m_μ/m_e

$$a_\mu^{\mathrm{QED}} - a_e^{\mathrm{QED}} = 619\,500.2 \times 10^{-11}$$

a_μ, QED and the SM

World Average (before FNAL)

$$a_\mu^{\text{exp}} = (116\,592\,089 \pm 63) \times 10^{-11}$$

- The bulk of the difference between a_e and a_μ is due to QED and originates from large logs of m_μ/m_e

$$a_\mu^{\text{QED}} - a_e^{\text{QED}} = 619\,500.2 \times 10^{-11}$$

$$a_\mu^{\text{exp}} - a_\mu^{\text{QED}} = (7360 \pm 63) \times 10^{-11}$$

a_μ, QED and the SM

World Average (before FNAL)

$$a_\mu^{\text{exp}} = (116\,592\,089 \pm 63) \times 10^{-11}$$

- The bulk of the difference between a_e and a_μ is due to QED and originates from large logs of m_μ/m_e

$$a_\mu^{\text{QED}} - a_e^{\text{QED}} = 619\,500.2 \times 10^{-11}$$
$$a_\mu^{\text{exp}} - a_\mu^{\text{QED}} = (7360 \pm 63) \times 10^{-11}$$

- Hadronic contributions are large

$$a_\mu^{\text{had}} \simeq 7000 \times 10^{-11}$$

"Seen" at the 5σ level already in 1979

a_μ, QED and the SM

World Average (before FNAL)

$$a_\mu^{\rm exp} = (116\,592\,089 \pm 63) \times 10^{-11}$$

- The bulk of the difference between a_e and a_μ is due to QED and originates from large logs of m_μ/m_e

$$a_\mu^{\rm QED} - a_e^{\rm QED} = 619\,500.2 \times 10^{-11}$$
$$a_\mu^{\rm exp} - a_\mu^{\rm QED} = (7360 \pm 63) \times 10^{-11}$$

- Hadronic contributions are large

$$a_\mu^{\rm had} \simeq 7000 \times 10^{-11}$$

  "Seen" at the 5σ level already in 1979
- Weak contributions to a_μ

$$a_\mu^{\rm EW} = 154 \times 10^{-11} \simeq 2.5 \Delta a_\mu^{\rm exp}$$

Present status of $(g-2)_\mu$: experiment vs SM

Before

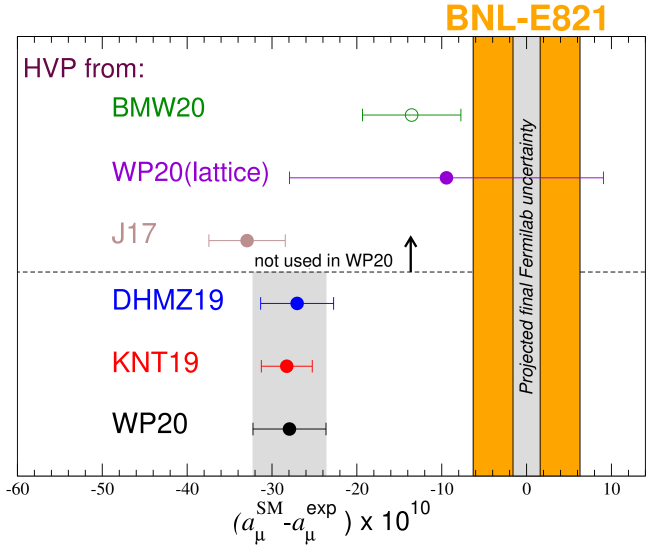

Present status of $(g-2)_\mu$: experiment vs SM

After the 2021 Fermilab result

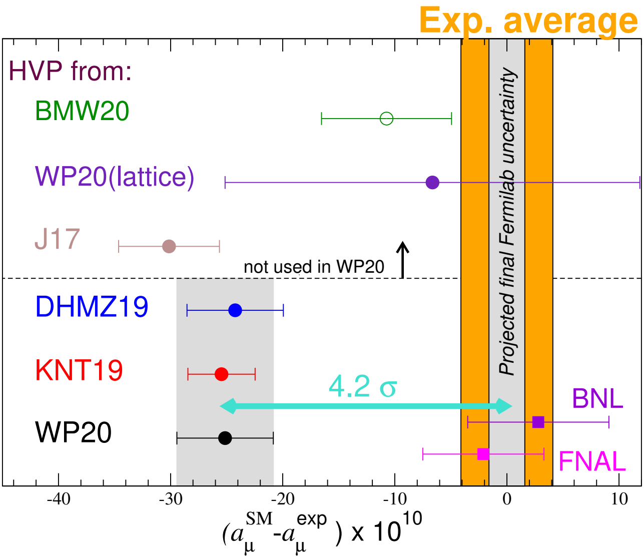

Present status of $(g-2)_\mu$: experiment vs SM

After the 2023 Fermilab result

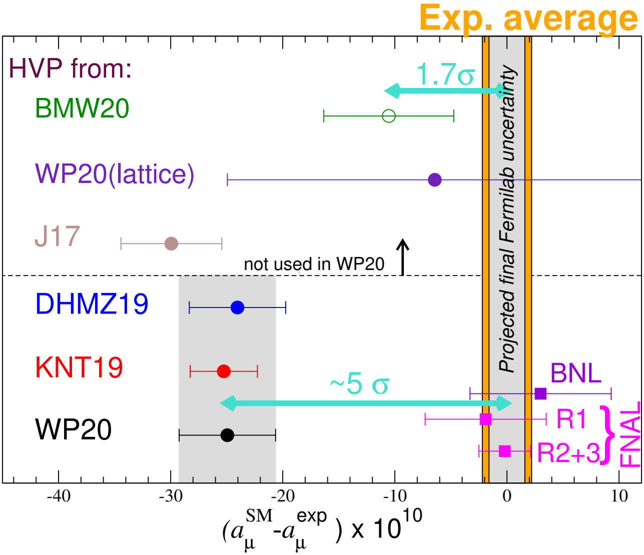

White Paper (2020): $(g-2)_\mu$, experiment vs SM

Contribution	Value $\times 10^{11}$
HVP LO (e^+e^-)	6931(40)
HVP NLO (e^+e^-)	$-98.3(7)$
HVP NNLO (e^+e^-)	12.4(1)
HVP LO (lattice , *udsc*)	7116(184)
HLbL (phenomenology)	92(19)
HLbL NLO (phenomenology)	2(1)
HLbL (lattice, *uds*)	79(35)
HLbL (phenomenology + lattice)	90(17)
QED	116 584 718.931(104)
Electroweak	153.6(1.0)
HVP (e^+e^-, LO + NLO + NNLO)	6845(40)
HLbL (phenomenology + lattice + NLO)	92(18)
Total SM Value	116 591 810(43)
Experiment	116 592 059(22)
Difference: $\Delta a_\mu := a_\mu^{\text{exp}} - a_\mu^{\text{SM}}$	249(48)

White Paper (2020): $(g-2)_\mu$, experiment vs SM

Contribution	Value $\times 10^{11}$
HVP LO (e^+e^-)	6931(40)
HVP NLO (e^+e^-)	$-98.3(7)$
HVP NNLO (e^+e^-)	12.4(1)
HVP LO (lattice BMW(20), *udsc*)	7075(55)
HLbL (phenomenology)	92(19)
HLbL NLO (phenomenology)	2(1)
HLbL (lattice, *uds*)	79(35)
HLbL (phenomenology + lattice)	90(17)
QED	116 584 718.931(104)
Electroweak	153.6(1.0)
HVP (e^+e^-, LO + NLO + NNLO)	6845(40)
HLbL (phenomenology + lattice + NLO)	92(18)
Total SM Value	116 591 810(43)
Experiment	116 592 059(22)
Difference: $\Delta a_\mu := a_\mu^{\text{exp}} - a_\mu^{\text{SM}}$	249(48)

White Paper (2020): $(g-2)_\mu$, experiment vs SM

White Paper:

T. Aoyama et al. Phys. Rep. 887 (2020) = WP(20)

Muon $g-2$ Theory Initiative

Steering Committee:

GC

Michel Davier (vice-chair)

Aida El-Khadra (chair)

Martin Hoferichter

Laurent Lellouch

Christoph Lehner (vice-chair)

Tsutomu Mibe (J-PARC E34 experiment)

Lee Roberts (Fermilab E989 experiment)

Thomas Teubner

Hartmut Wittig

White Paper (2020): $(g-2)_\mu$, experiment vs SM

White Paper:
T. Aoyama et al. Phys. Rep. 887 (2020) = WP(20)

Muon $g-2$ Theory Initiative
Workshops:

- 1st plenary meeting, Q-Center (Fermilab), 3-6 June 2017
- HVP WG workshop, KEK (Japan), 12-14 February 2018
- HLbL WG workshop, U. of Connecticut, 12-14 March 2018
- 2nd plenary meeting, Mainz, 18-22 June 2018
- 3rd plenary meeting, Seattle, 9-13 September 2019
- Lattice HVP workshop, virtual, 16-20 November 2020
- 4th plenary meeting, KEK (virtual), 28 June-02 July 2021
- 5th plenary meeting, Higgs Center Edinburgh, 5-9 Sept. 2022
- 6th plenary meeting, Bern, 4-8 Sept. 2023

White Paper executive summary (my own)

- QED and EW known and stable, negligible uncertainties
- HVP dispersive: consensus number, conservative uncertainty (KNT19, DHMZ19, CHS19, HHK19)
- HVP lattice: consensus number, $\Delta a_\mu^{\rm HVP,latt} \sim 5\,\Delta a_\mu^{\rm HVP,disp}$ (Fermilab-HPQCD-MILC18,20, BMW18, RBC/UKQCD18, ETM19,SK19, Mainz19, ABTGJP20)
- HVP BMW20: central value $\to$ discrepancy $< 2\sigma$; $\Delta a_\mu^{\rm HVP,BMW} \sim \Delta a_\mu^{\rm HVP,disp}$ published 04/21 $\to$ not in WP
- HLbL dispersive: consensus number, w/ recent improvements $\Rightarrow$ $\Delta a_\mu^{\rm HLbL} \sim 0.5\,\Delta a_\mu^{\rm HVP}$
- HLbL lattice: single calculation, agrees with dispersive ($\Delta a_\mu^{\rm HLbL,latt} \sim 2\,\Delta a_\mu^{\rm HLbL,disp}$) $\to$ final average (RBC/UKQCD20)

Theory uncertainty comes from hadronic physics

- Hadronic contributions responsible for most of the theory uncertainty
- Hadronic vacuum polarization (HVP) is $\mathcal{O}(\alpha^2)$, dominates the total uncertainty, despite being known to $< 1\%$

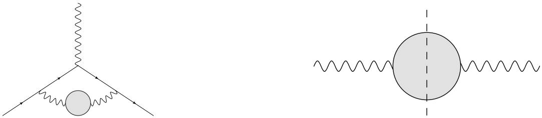

- unitarity and analyticity $\Rightarrow$ dispersive approach
- $\Rightarrow$ direct relation to experiment: $\sigma_{\text{tot}}(e^+e^- \to \text{hadrons})$
- e^+e^- Exps: BaBar, Belle, BESIII, CMD2/3, KLOE2, SND
- alternative approach: lattice, becoming competitive

(BMW, ETMC, Fermilab, HPQCD, Mainz, MILC, RBC/UKQCD)

Theory uncertainty comes from hadronic physics

- Hadronic contributions responsible for most of the theory uncertainty
- Hadronic vacuum polarization (HVP) is $\mathcal{O}(\alpha^2)$, dominates the total uncertainty, despite being known to $< 1\%$
- Hadronic light-by-light (HLbL) is $\mathcal{O}(\alpha^3)$, known to $\sim 20\%$, second largest uncertainty (now subdominant)

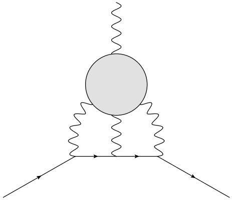

- earlier: model-based—uncertainties difficult to quantify
- recently: dispersive approach $\Rightarrow$ data-driven, systematic treatment
- lattice QCD is becoming competitive

(Mainz, RBC/UKQCD)

Outline

HLbL contribution: Master Formula

$$a_\mu^{\mathrm{HLbL}} = \frac{2\alpha^3}{48\pi^2} \int_0^\infty dQ_1 \int_0^\infty dQ_2 \int_{-1}^{1} d\tau \sqrt{1-\tau^2} \sum_{i=1}^{12} T_i(Q_1, Q_2, \tau) \bar{\Pi}_i(Q_1, Q_2, \tau)$$

Q_i^μ are the Wick-rotated four-momenta and τ the four-dimensional angle between Euclidean momenta:

$$Q_1 \cdot Q_2 = |Q_1||Q_2|\tau$$

The integration variables $Q_1 := |Q_1|$, $Q_2 := |Q_2|$.

GC, Hoferichter, Procura, Stoffer (15)

- T_i: known kernel functions
- $\bar{\Pi}_i$ are amenable to a dispersive treatment:
  imaginary parts are related to measurable subprocesses

Improvements obtained with the dispersive approach

Contribution	PdRV(09) *Glasgow consensus*	N/JN(09)	J(17)	WP(20)
π^0, η, η'-poles	114(13)	99(16)	95.45(12.40)	93.8(4.0)
π, K-loops/boxes	$-19(19)$	$-19(13)$	$-20(5)$	$-16.4(2)$
S-wave $\pi\pi$ rescattering	$-7(7)$	$-7(2)$	$-5.98(1.20)$	$-8(1)$
subtotal	88(24)	73(21)	69.5(13.4)	69.4(4.1)
scalars	–	–	–	$-1(3)$
tensors	–	–	1.1(1)	
axial vectors	15(10)	22(5)	7.55(2.71)	6(6)
u, d, s-loops / short-distance	–	21(3)	20(4)	15(10)
c-loop	2.3	–	2.3(2)	3(1)
total	105(26)	116(39)	100.4(28.2)	92(19)

- significant reduction of uncertainties in the first three rows

  CHPS (17), Masjuan, Sánchez-Puertas (17) Hoferichter, Hoid et al. (18), Gerardin, Meyer, Nyffeler (19)

- Resonances affected by basis ambiguity and large uncertainties

  Danilkin, Hoferichter, Stoffer (21)

  New promising approach solves this — Lüdtke, Procura, Stoffer (23)

- asymptotic region recently addressed, — Melnikov, Vainshtein (04), Nyffeler (09)

  WP20, GC, Hagelstein et al. (21)

  still work in progress — Bijnens et al. (20,21), Cappiello et al. (20), Leutgeb, Rebhan (19,21)

Situation for HLbL

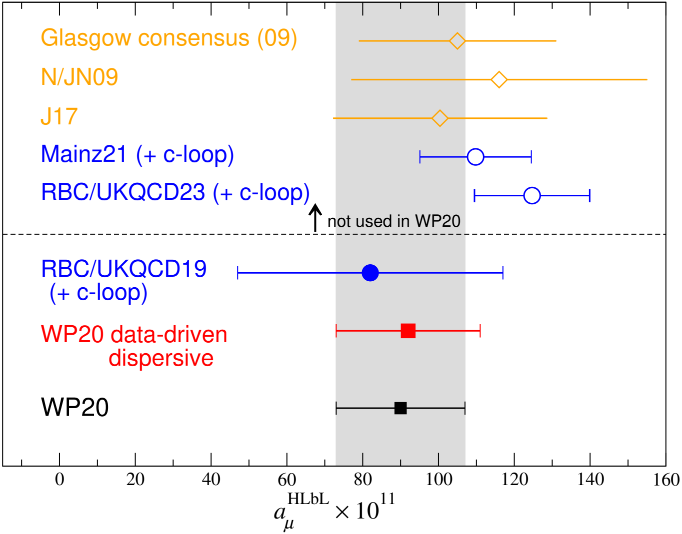

Outline

Introduction: $(g-2)_\mu$ in the Standard Model

Hadronic light-by-light

Hadronic Vacuum Polarization contribution

- Data-driven approach
- Lattice vs data-driven: intermediate window
- The MUonE experiment
- Radiative corrections with a dispersive approach: A_{FB} and σ

Conclusions and Outlook

HVP contribution: Master Formula

Unitarity relation: simple, same for all intermediate states

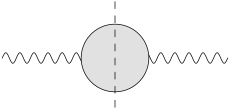

$$\mathrm{Im}\bar{\Pi}(q^2) \propto \sigma(e^+e^- \to \text{hadrons}) = \sigma(e^+e^- \to \mu^+\mu^-)R(q^2)$$

Analyticity $\left[\bar{\Pi}(q^2) = \frac{q^2}{\pi}\int ds \frac{\mathrm{Im}\bar{\Pi}(s)}{s(s-q^2)}\right] \Rightarrow$ Master formula for HVP

Bouchiat, Michel (61)

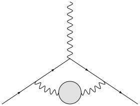

$$\Leftrightarrow \qquad a_\mu^{\text{hvp}} = \frac{\alpha^2}{3\pi^2}\int_{s_{th}}^{\infty} \frac{ds}{s} K(s)R(s)$$

$K(s)$ known, depends on m_μ and $K(s) \sim \frac{1}{s}$ for large s

Comparison between DHMZ19 and KNT19

	DHMZ19	KNT19	Difference
$\pi^+\pi^-$	507.85(0.83)(3.23)(0.55)	504.23(1.90)	3.62
$\pi^+\pi^-\pi^0$	46.21(0.40)(1.10)(0.86)	46.63(94)	-0.42
$\pi^+\pi^-\pi^+\pi^-$	13.68(0.03)(0.27)(0.14)	13.99(19)	-0.31
$\pi^+\pi^-\pi^0\pi^0$	18.03(0.06)(0.48)(0.26)	18.15(74)	-0.12
K^+K^-	23.08(0.20)(0.33)(0.21)	23.00(22)	0.08
K_SK_L	12.82(0.06)(0.18)(0.15)	13.04(19)	-0.22
$\pi^0\gamma$	4.41(0.06)(0.04)(0.07)	4.58(10)	-0.17
Sum of the above	626.08(0.95)(3.48)(1.47)	623.62(2.27)	2.46
$[1.8, 3.7]$ GeV (without $c\bar{c}$)	33.45(71)	34.45(56)	-1.00
J/ψ, $\psi(2S)$	7.76(12)	7.84(19)	-0.08
$[3.7, \infty)$ GeV	17.15(31)	16.95(19)	0.20
Total $a_\mu^{\text{HVP, LO}}$	$694.0(1.0)(3.5)(1.6)(0.1)_\psi(0.7)_{\text{DV+QCD}}$	692.8(2.4)	1.2

Comparison between DHMZ19 and KNT19

	DHMZ19	KNT19	Difference
$\pi^+\pi^-$	507.85(0.83)(3.23)(0.55)	504.23(1.90)	3.62
$\pi^+\pi^-\pi^0$	46.21(0.40)(1.10)(0.86)	46.63(94)	-0.42
$\pi^+\pi^-\pi^+\pi^-$	13.68(0.03)(0.27)(0.14)	13.99(19)	-0.31
$\pi^+\pi^-\pi^0\pi^0$	18.03(0.06)(0.48)(0.26)	18.15(74)	-0.12
K^+K^-	23.08(0.20)(0.33)(0.21)	23.00(22)	0.08
K_SK_L	12.82(0.06)(0.18)(0.15)	13.04(19)	-0.22
$\pi^0\gamma$	4.41(0.06)(0.04)(0.07)	4.58(10)	-0.17
Sum of the above	626.08(0.95)(3.48)(1.47)	623.62(2.27)	2.46
$[1.8, 3.7]\,\mathrm{GeV}$ (without $c\bar{c}$)	33.45(71)	34.45(56)	-1.00
J/ψ, $\psi(2S)$	7.76(12)	7.84(19)	-0.08
$[3.7, \infty)\,\mathrm{GeV}$	17.15(31)	16.95(19)	0.20
Total $a_\mu^{\text{HVP, LO}}$	$694.0(1.0)(3.5)(1.6)(0.1)_\psi(0.7)_{\mathrm{DV+QCD}}$	692.8(2.4)	1.2

For the dominant $\pi\pi$ channel more theory input can be used

Omnès representation including isospin breaking

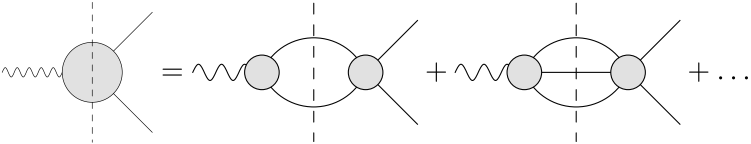

Omnès representation including isospin breaking

- Omnès representation

$$F_\pi^V(s) = \exp\left[\frac{s}{\pi}\int_{4M_\pi^2}^{\infty} ds' \frac{\delta(s')}{s'(s'-s)}\right] \equiv \Omega(s)$$

- Split elastic ($\leftrightarrow \pi\pi$ phase shift, δ_1^1) from inelastic phase

$$\delta = \delta_1^1 + \delta_{\rm in} \quad \Rightarrow \quad F_\pi^V(s) = \Omega_1^1(s)\Omega_{\rm in}(s)$$

Eidelman-Lukaszuk: unitarity bound on $\delta_{\rm in}$

$$\sin^2\delta_{\rm in} \leq \frac{1}{2}\left(1-\sqrt{1-r^2}\right), \quad r = \frac{\sigma^{I=1}_{e^+e^-\to\neq 2\pi}}{\sigma_{e^+e^-\to 2\pi}} \Rightarrow s_{\rm in} = (M_\pi + M_\omega)^2$$

- $\rho-\omega$–mixing $\qquad F_V(s) = \Omega_{\pi\pi}(s)\cdot\Omega_{\rm in}(s)\cdot G_\omega(s)$

$$G_\omega(s) = 1 + \epsilon\frac{s}{s_\omega - s} \qquad \text{where} \qquad s_\omega = (M_\omega - i\Gamma_\omega/2)^2$$

Fit results

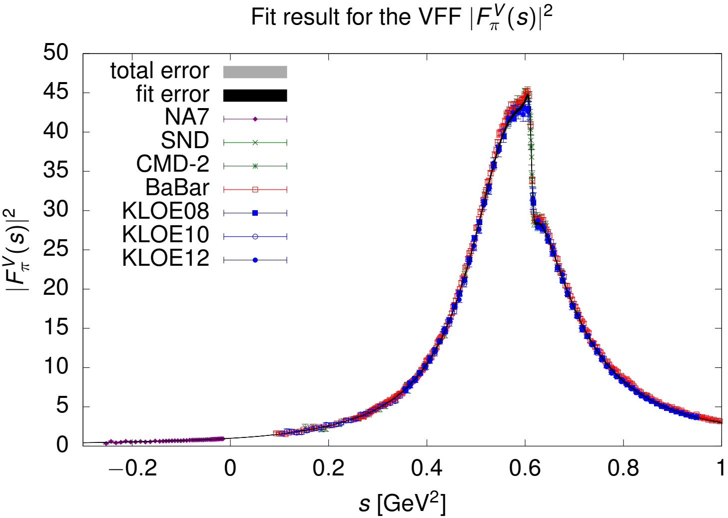
Fit result for the VFF $|F_\pi^V(s)|^2$
$|F_\pi^V(s)|^2$
s [GeV^2]
total error
fit error
NA7
SND
CMD-2
BaBar
KLOE08
KLOE10
KLOE12
50
45
40
35
30
25
20
15
10
5
0
−0.2
0
0.2
0.4
0.6
0.8
1

Fit results

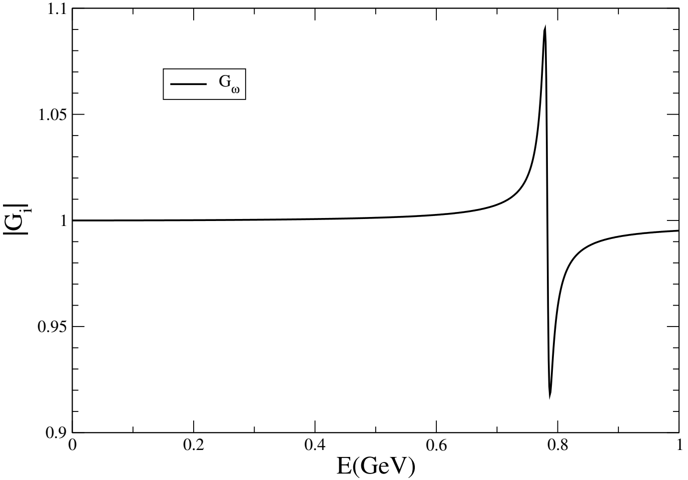

Fit results

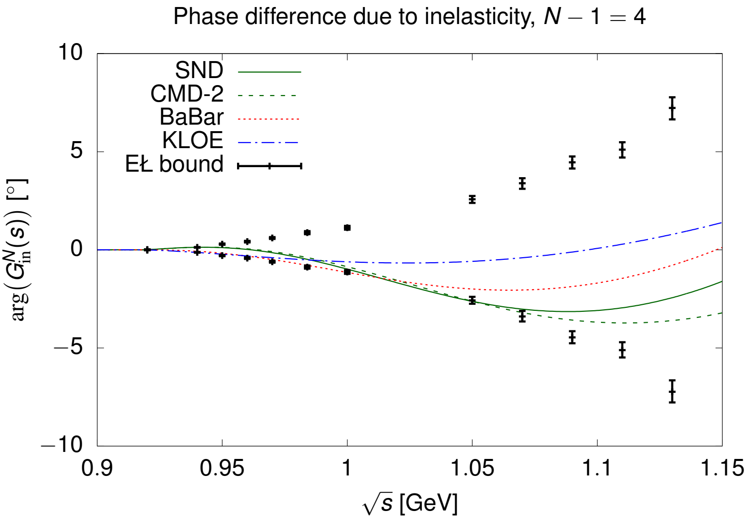
Phase difference due to inelasticity, $N-1=4$
SND
CMD-2
BaBar
KLOE
EŁ bound
$\arg\left(G_{\mathrm{in}}^N(s)\right)$ [°]
$\sqrt{s}$ [GeV]
10
5
0
−5
−10
0.9
0.95
1
1.05
1.1
1.15

Fit results

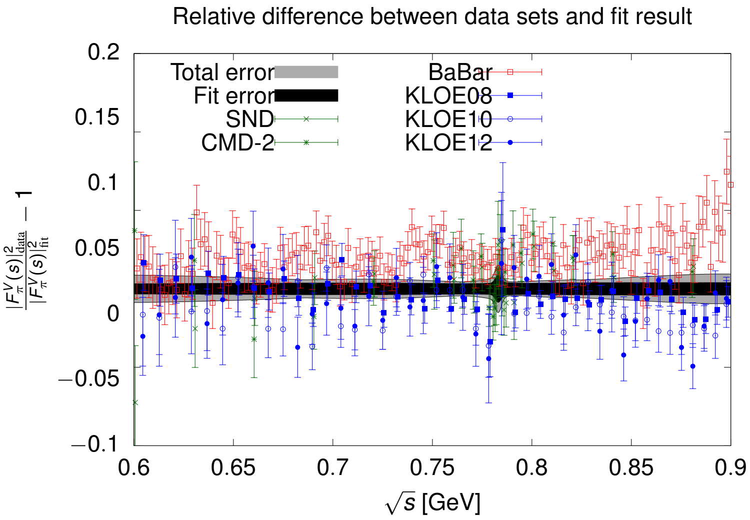
Relative difference between data sets and fit result
Total error
Fit error
SND
CMD-2
BaBar
KLOE08
KLOE10
KLOE12
$\frac{|F_\pi^V(s)|^2_{\text{data}}}{|F_\pi^V(s)|^2_{\text{fit}}} - 1$
0.2
0.15
0.1
0.05
0
−0.05
−0.1
0.6
0.65
0.7
0.75
0.8
0.85
0.9
$\sqrt{s}$ [GeV]

Fit results

Result for $a_\mu^{\pi\pi}|_{\leq 1\,\mathrm{GeV}}$ from the VFF fits to single experiments and combinations

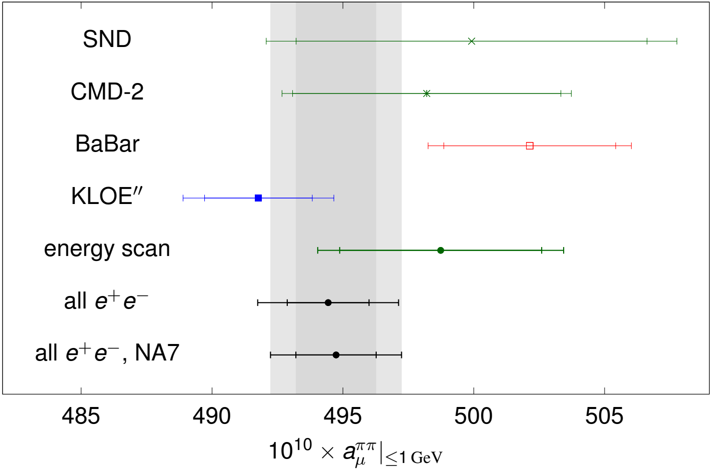

2π: comparison with the dispersive approach

The 2π channel can itself be described dispersively $\Rightarrow$ more constrained theoretically

Ananthanarayan, Caprini, Das (19), GC, Hoferichter, Stoffer (18)

Energy range	ACD18	CHS18	DHMZ19	KNT19
$\leq 0.6\,\mathrm{GeV}$		110.1(9)	110.4(4)(5)	108.7(9)
$\leq 0.7\,\mathrm{GeV}$		214.8(1.7)	214.7(0.8)(1.1)	213.1(1.2)
$\leq 0.8\,\mathrm{GeV}$		413.2(2.3)	414.4(1.5)(2.3)	412.0(1.7)
$\leq 0.9\,\mathrm{GeV}$		479.8(2.6)	481.9(1.8)(2.9)	478.5(1.8)
$\leq 1.0\,\mathrm{GeV}$		495.0(2.6)	497.4(1.8)(3.1)	493.8(1.9)
$[0.6, 0.7]\,\mathrm{GeV}$		104.7(7)	104.2(5)(5)	104.4(5)
$[0.7, 0.8]\,\mathrm{GeV}$		198.3(9)	199.8(0.9)(1.2)	198.9(7)
$[0.8, 0.9]\,\mathrm{GeV}$		66.6(4)	67.5(4)(6)	66.6(3)
$[0.9, 1.0]\,\mathrm{GeV}$		15.3(1)	15.5(1)(2)	15.3(1)
$\leq 0.63\,\mathrm{GeV}$	132.9(8)	132.8(1.1)	132.9(5)(6)	131.2(1.0)
$[0.6, 0.9]\,\mathrm{GeV}$		369.6(1.7)	371.5(1.5)(2.3)	369.8(1.3)
$\left[\sqrt{0.1}, \sqrt{0.95}\,\right]\,\mathrm{GeV}$		490.7(2.6)	493.1(1.8)(3.1)	489.5(1.9)

WP(20)

Combination method and final result

Complete analyses DHMZ19 and KNT19, as well as CHS19 (2π) and HHK19 (3π), have been so combined:

- central values are obtained by simple averages (for each channel and mass range)
- the largest experimental and systematic uncertainty of DHMZ and KNT is taken
- $1/2$ difference DHMZ$-$KNT (or BABAR$-$KLOE in the 2π channel, if larger) is added to the uncertainty

Final result:

$$
\begin{aligned}
a_\mu^{\text{HVP, LO}} &= 693.1(2.8)_{\text{exp}}(2.8)_{\text{sys}}(0.7)_{\text{DV+QCD}} \times 10^{-10} \\
&= 693.1(4.0) \times 10^{-10}
\end{aligned}
$$

WP(20)

The BMW result

Borsanyi et al. Nature 2021

State-of-the-art lattice calculation of $a_\mu^{\text{HVP, LO}}$ based on

- current-current correlator, summed over all distances, integrated in time with appropriate kernel function (TMR)
- using staggered fermions on an $L \sim 6$ fm lattice ($L \sim 11$fm used for finite volume corrections)
- at (and around) physical quark masses
- including isospin-breaking effects

The BMW result

Borsanyi et al. Nature 2021

Isospin-symmetric

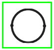

Connected light

$633.7(2.1)_{stat}(4.2)_{syst}$

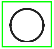

Connected strange

$53.393(89)_{stat}(68)_{syst}$

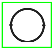

Connected charm

$14.6(0)_{stat}(1)_{syst}$

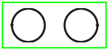

Disconnected

$-13.36(1.18)_{stat}(1.36)_{syst}$

QED isospin breaking: valence

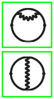

Connected $-1.23(40)_{stat}(31)_{syst}$

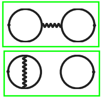

Disconnected $-0.55(15)_{stat}(10)_{syst}$

Strong–isospin breaking

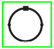

Connected

$6.60(63)_{stat}(53)_{syst}$

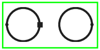

Disconnected

$-4.67(54)_{stat}(69)_{syst}$

QED isospin breaking: sea

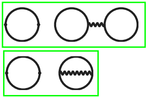

Connected $0.37(21)_{stat}(24)_{syst}$

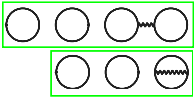

Disconnected $-0.040(33)_{stat}(21)_{syst}$

Other

Bottom; higher-order; perturbative

$0.11(4)_{tot}$

QED isospin breaking: mixed

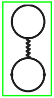

Connected $-0.0093(86)_{stat}(95)_{syst}$

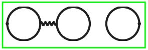

Disconnected $0.011(24)_{stat}(14)_{syst}$

Finite-size effects

Isospin-symmetric

$18.7(2.5)_{tot}$

Isospin-breaking

$0.0(0.1)_{tot}$

$$a_\mu^{\text{LO-HVP}}\ (\times 10^{10}) = 707.5(2.3)_{stat}(5.0)_{syst}(5.5)_{tot}$$

The BMW result

Borsanyi et al. Nature 2021

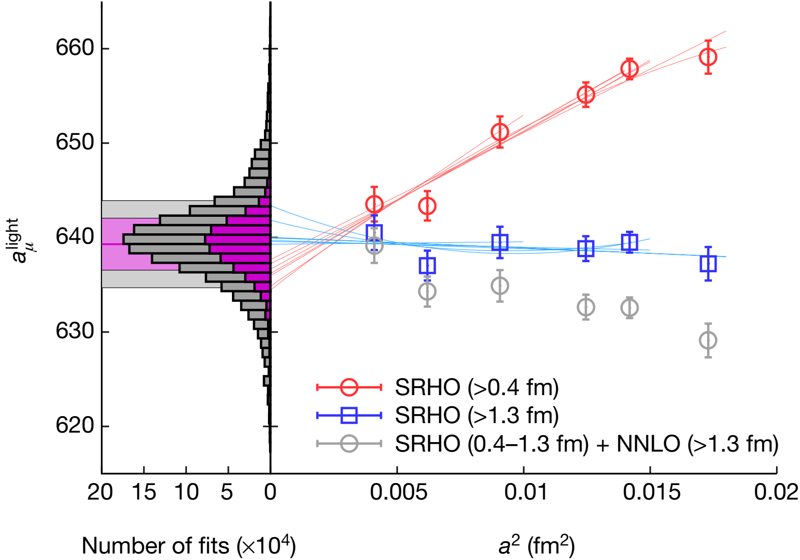

The BMW result

Borsanyi et al. Nature 2021

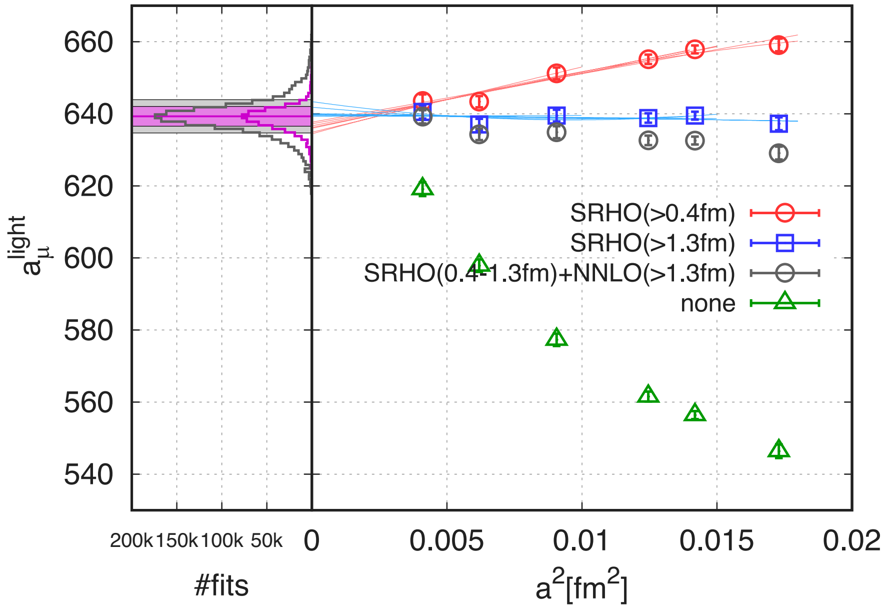

The BMW result

Borsanyi et al. Nature 2021

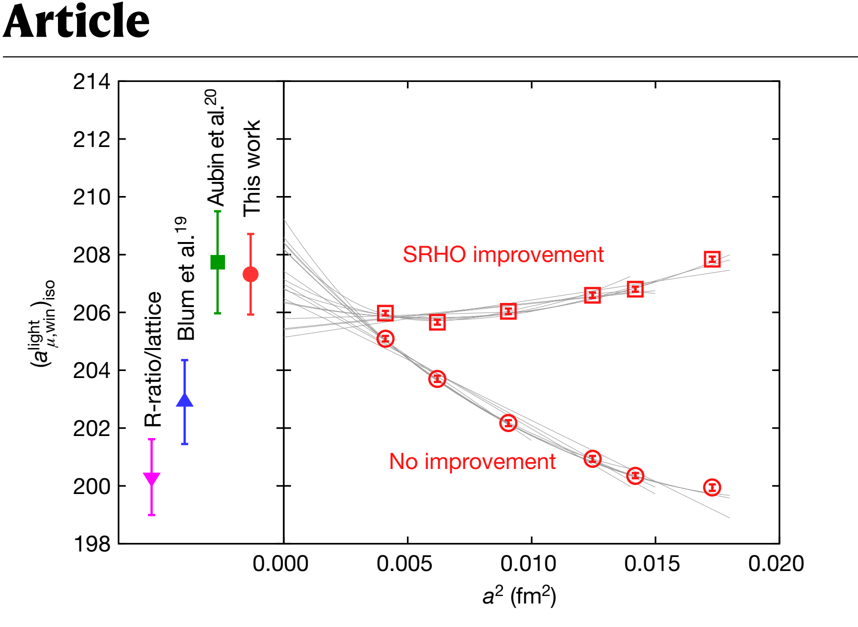

The BMW result

Borsanyi et al. Nature 2021

Weight functions for window quantities

RBC/UKQCD (18)

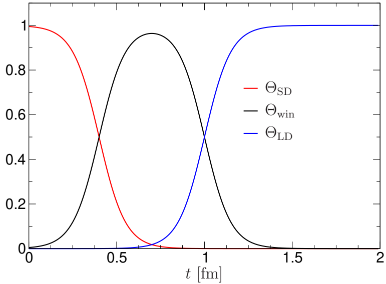

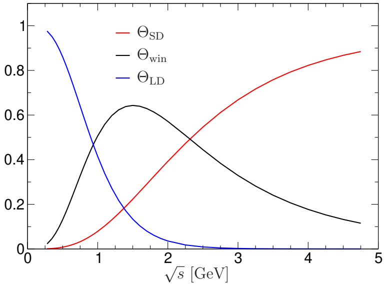

Present status of the window quantities

Lattice calculations of a_μ^{win}, circa 2021

Summary: *ud* contribution

f	$a_\mu^{SD}(f)\cdot 10^{10}$	$a_\mu^{W}(f)\cdot 10^{10}$	$a_\mu^{LD}(f)\cdot 10^{10}$
ud	48.2 (0.8)	202.2 (2.6)	382.5 (11.7)

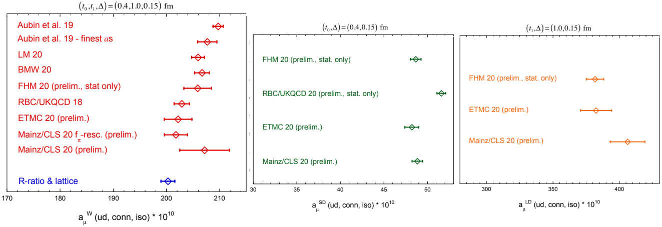

13

D. Giusti, talk at Lattice 2021

Present status of the window quantities

Now several lattice calculations confirm BMW's result

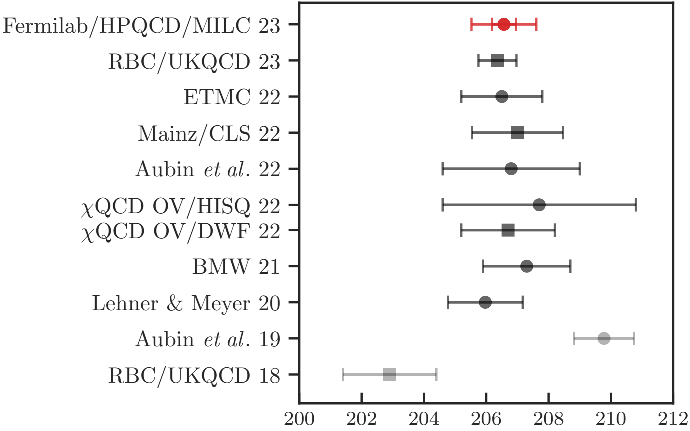

arXiv:2301.08274, Fermilab Lattice-HPQCD-MILC (23)

Present status of the window quantities

Now several lattice calculations confirm BMW's result

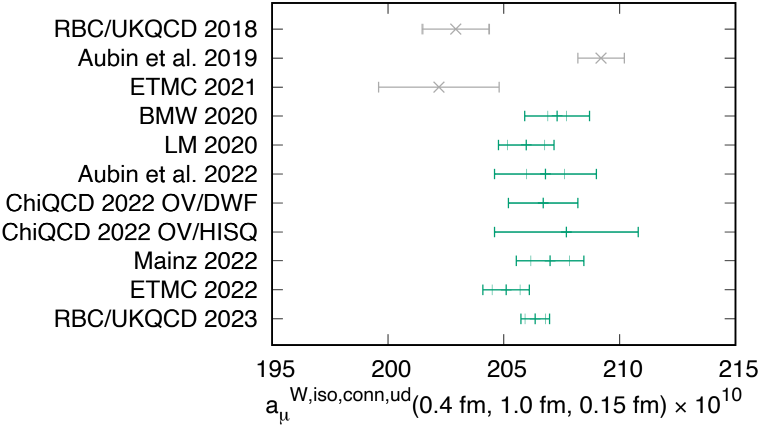

arXiv:2301.08696 RBC/UKQCD (23)

Present status of the window quantities

Now several lattice calculations confirm BMW's result

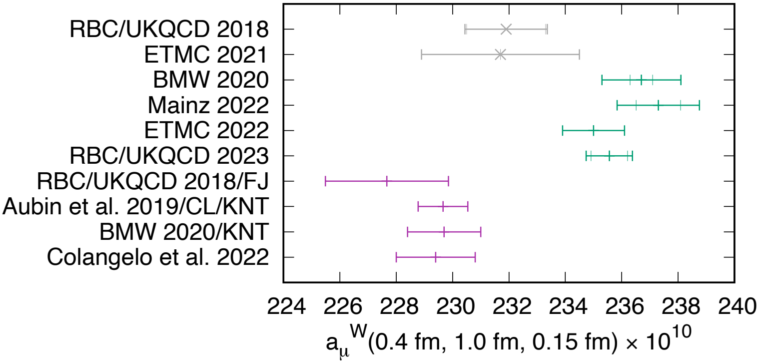

arXiv:2301.08696 RBC/UKQCD (23)

Individual-channel contributions to a_μ^{win}

Channel	total	window
$\pi^+\pi^-$	504.23(1.90)	144.08(49)
$\pi^+\pi^-\pi^0$	46.63(94)	18.63(35)
$\pi^+\pi^-\pi^+\pi^-$	13.99(19)	8.88(12)
$\pi^+\pi^-\pi^0\pi^0$	18.15(74)	11.20(46)
K^+K^-	23.00(22)	12.29(12)
$K_S K_L$	13.04(19)	6.81(10)
$\pi^0\gamma$	4.58(10)	1.58(4)
Sum of the above	623.62(2.27)	203.47(78)
$[1.8, 3.7]$ GeV (without $c\bar{c}$)	34.45(56)	15.93(26)
J/ψ, $\psi(2S)$	7.84(19)	2.27(6)
$[3.7, \infty)$ GeV	16.95(19)	1.56(2)
WP(20) / GC, El-Khadra *et al.* (22)	693.1(4.0)	229.4(1.4)
BMWc	707.5(5.5)	236.7(1.4)
Mainz/CLS		237.3(1.5)
ETMc		235.0(1.1)
RBC/UKQCD		235.6(0.8)

Numbers for the channels refer to KNT19 — thanks to Alex Keshavarzi for providing them

$$\Delta a_\mu^{\text{HVP, LO}} = 14.4(6.8)\,(2.1\sigma), \qquad \Delta a_\mu^{\text{win}} \sim 6.5(1.5)\,(\sim 4.3\sigma)$$

CMD-3 measurement of $e^+e^- \to \pi^+\pi^-$

F. Ignatov et al., CMD-3, arXiv:2302.08834

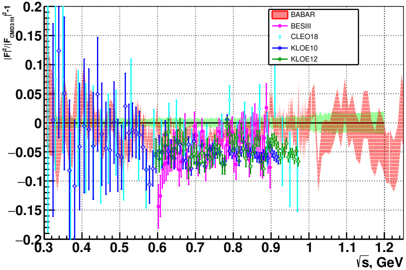

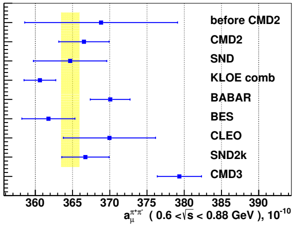

The comparison of pion form factor measured in this work with the most recent ISR experiments (BABAR [21], KLOE [18, 19], BES [22]) is shown in Fig. 34. The comparison with the most precise previous energy scan experiments (CMD-2 [12, 13, 14, 15], SND [16] at the VEPP-2M and SND [23] at the VEPP-2000) is shown in Fig. 35. The new result generally shows larger pion form factor in the whole energy range under discussion. The most significant difference to other energy scan measurements, including previous CMD-2 measurement, is observed at the left side of ρ-meson ($\sqrt{s} = 0.6 - 0.75$ GeV), where it reach up to 5%, well beyond the combined systematic and statistical errors of the new and previous results. The source of this difference is unknown at the moment.

Preliminary analysis of the CMD-3 measurement

Work in progress, GC, Hoferichter and Stoffer (thanks for providing the plots)

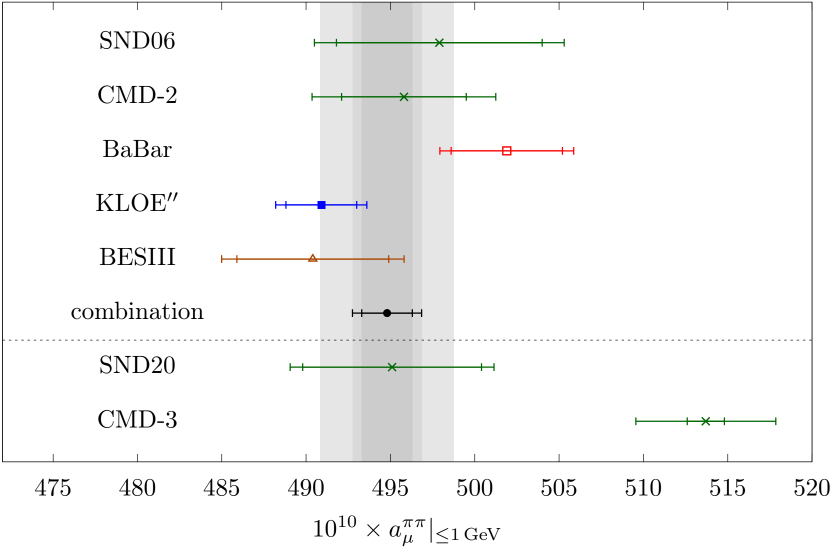

Preliminary analysis of the CMD-3 measurement

Work in progress, GC, Hoferichter and Stoffer (thanks for providing the plots)

$10^{10}\times$	$a_\mu^{\pi\pi}\|_{\leq 1\mathrm{GeV}}$	$a_\mu^{\pi\pi,\mathrm{win}}\|_{\leq 1\mathrm{GeV}}$	χ^2/dof
SND06	497.9(6.1)(4.2)	139.6(1.8)(1.0)	1.09
CMD-2	495.8(3.7)(4.0)	139.4(1.0)(0.8)	1.01
BaBar	501.9(3.3)(2.2)	140.6(1.0)(0.7)	1.17
KLOE”	490.9(2.1)(1.7)	137.1(0.6)(0.4)	1.13
BESIII	490.4(4.5)(3.0)	137.8(1.3)(0.4)	1.01
SND20	495.1(5.3)(2.9)	139.2(1.5)(0.4)	1.88
CMD-3	513.7(1.1)(4.0)	144.0(0.3)(1.1)	1.09
Combination	494.8(1.5)(1.4)(3.4)	138.3(0.4)(0.3)(1.1)	1.21

Combination: NA7 + all data sets other than SND20 and CMD-3

$$\Delta a_\mu^{\text{HVP, LO}}(\text{CMD-3-Comb.}) = 18.9(5.1)\,, \qquad \Delta a_\mu^{\mathrm{win}}(\text{CMD-3-Comb.}) = 5.7(1.5)$$

$$\Delta a_\mu^{\text{HVP, LO}}(\text{BMW-WP20}) = 14.4(6.8), \qquad \Delta a_\mu^{\mathrm{win}}(\text{Lattice-WP20}) \sim 6.5(1.5)$$

MUonE

Measure $\mu e \to \mu e$ scattering, *i.e.* $\bar{\Pi}(q^2)$ for $q^2 < 0$

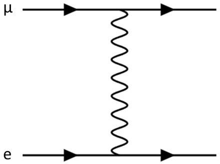

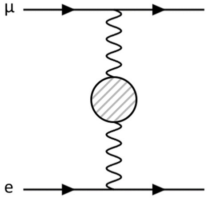

related by analyticity to $\bar{\Pi}(q^2)$ for $q^2 > 0$:

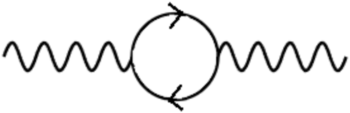

MUonE

Switching from time- to spacelike for $\Pi(s)$:

$$a_\mu^{\text{HVP, LO}} = \frac{\alpha}{\pi^2}\int_{s_{th}}^{\infty} ds \frac{K(s)}{s}\mathrm{Im}\bar{\Pi}(s) = -\frac{\alpha}{\pi}\int_0^1 dx(1-x)\bar{\Pi}(t(x))$$

where

$$t(x) = -\frac{x^2 m_\mu^2}{1-x}$$

MUonE

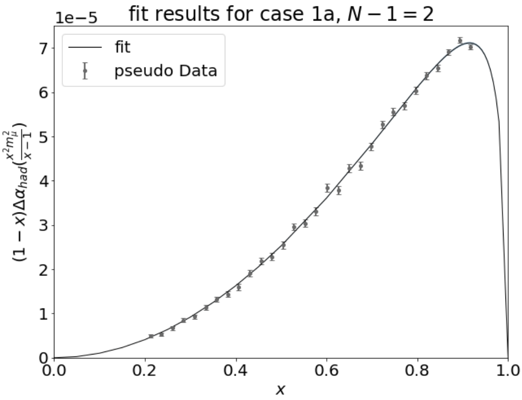

Pseudo data in range $0.21 < x < 0.92$.

Master Thesis of Barbara Jenny

See also: Greynat, de Rafael (22), Ignatov, Pilato, Teubner, Venanzoni (23)

MUonE

Pros:

- $\bar{\Pi}(q^2)$ very smooth for $q^2 < 0$
- $-\infty < q^2 \leq 0 \Leftrightarrow$ measurement in a finite range
- one single, compact experiment can determine $a_\mu^{\text{HVP, LO}}$

Cons:

- $|\bar{\Pi}_{\rm had}(q^2)| \ll |\bar{\Pi}_{\rm lept}(q^2)|$
- 1% for $\bar{\Pi}_{\rm had}(q^2)$ requires $\sim 10^{-5}$ for $\sigma(\mu e \to \mu e)$
- CERN schedule $\Rightarrow$ no results of needed precision < 6 yrs

Radiative corrections to $e^+e^- \to \pi^+\pi^-$

Initial State Radiation:

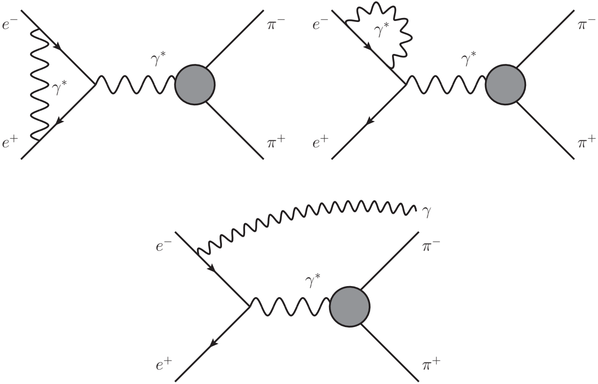

can be calculated in QED in terms of $F_\pi^V(s)$ (ISR based on this)

Radiative corrections to $e^+e^- \to \pi^+\pi^-$

Final State Radiation:

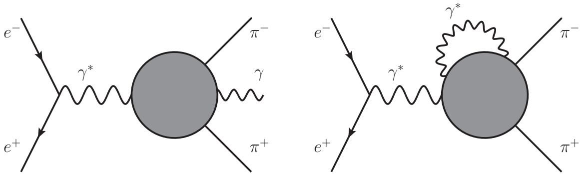

requires hadronic matrix elements beyond $F_\pi^V(s)$
known in ChPT to one loop

Kubis, Meißner (01)

Radiative corrections to $e^+e^- \to \pi^+\pi^-$

Interference terms:

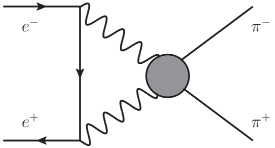

also require hadronic matrix elements beyond $F_\pi^V(s)$

Radiative corrections to $e^+e^- \to \pi^+\pi^-$

Interference terms:

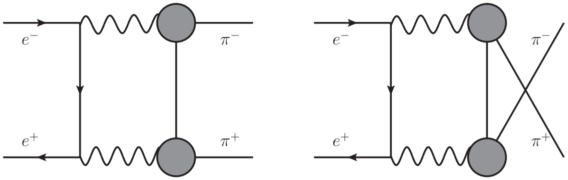

also require hadronic matrix elements beyond $F_\pi^V(s)$
other than in the 1π-exchange approximation;

do not contribute to the total cross section because C-odd
but to the forward-backward asymmetry

Forward-backward asymmetry

$$\frac{d\sigma_0}{dz} = \frac{\pi\alpha^2\beta^3}{4s}(1-z^2)\left|F_\pi^V(s)\right|^2, \qquad \beta = \sqrt{1-\frac{4M_\pi^2}{s}}, \qquad z = \cos\theta$$

$$A_{\text{FB}}(z) = \frac{\frac{d\sigma}{dz}(z) - \frac{d\sigma}{dz}(-z)}{\frac{d\sigma}{dz}(z) + \frac{d\sigma}{dz}(-z)}$$

$$\left.\frac{d\sigma}{dz}\right|_{C\text{-odd}} = \frac{d\sigma_0}{dz}\left[\delta_{\text{soft}}(m_\gamma^2,\Delta) + \delta_{\text{virt}}(m_\gamma^2)\right] + \left.\frac{d\sigma}{dz}\right|_{\text{hard}}(\Delta)$$

$$\delta_{\text{soft}} = \frac{2\alpha}{\pi}\left\{\log\frac{m_\gamma^2}{4\Delta^2}\log\frac{1+\beta z}{1-\beta z} + \log(1-\beta^2)\log\frac{1+\beta z}{1-\beta z} + \ldots\right\}$$

Calculation of δ_{virt} in the 1π-exchange approximation

- cut the diagrams in the t (or u) channel

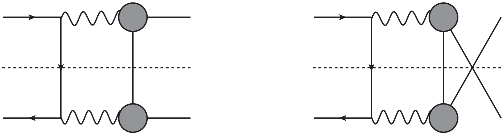

- represent the subamplitude $e^+e^- \to \pi^+\pi^-$ dispersively

$$\frac{F_\pi^V(s)}{s} = \frac{1}{s - m_\gamma^2} - \frac{1}{\pi}\int_{4M_\pi^2}^\infty ds' \frac{\mathrm{Im} F_\pi^V(s')}{s'} \frac{1}{s-s'}$$

- which leads to

GC, Hoferichter, Monnard, Ruiz de Elvira (22)

$$\delta_{\text{virt}} = \bar{\delta}_{\text{virt}}(m_\gamma^2, m_\gamma^2) - \frac{1}{\pi}\int_{4M_\pi^2}^\infty ds' \frac{\mathrm{Im} F_\pi^V(s')}{s'}\left[\bar{\delta}_{\text{virt}}(s', m_\gamma^2) + \bar{\delta}_{\text{virt}}(m_\gamma^2, s')\right]$$
$$+ \frac{1}{\pi}\int_{4M_\pi^2}^\infty ds' \frac{\mathrm{Im} F_\pi^V(s')}{s'} \frac{1}{\pi}\int_{4M_\pi^2}^\infty ds'' \frac{\mathrm{Im} F_\pi^V(s'')}{s''} \bar{\delta}_{\text{virt}}(s', s''),$$

Numerical analysis

GC, Hofericher, Monnard, Ruiz de Elvira (22)

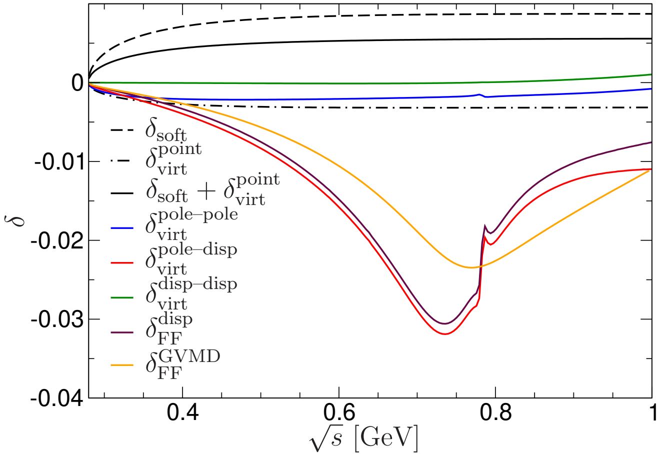

GVMD describes well CMD3 data

Ignatov, Lee (22), CMD-3 (23)

Numerical analysis

GC, Hoferichter, Monnard, Ruiz de Elvira (22)

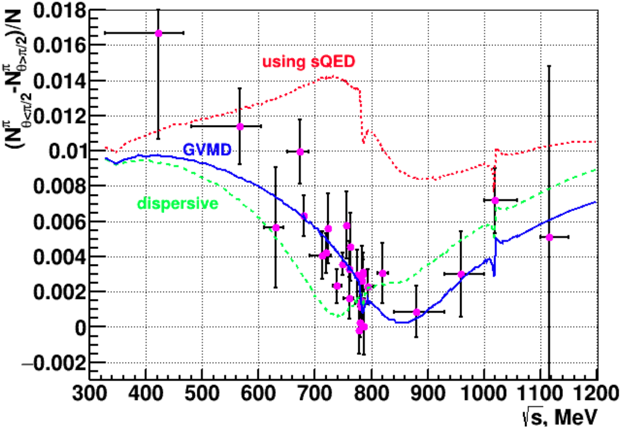

Figure courtesy of F. Ignatov

Dispersive treatment of FSR in $e^+e^- \to \pi^+\pi^-$

$$\begin{aligned}\frac{\mathrm{Disc}F_\pi^{V,\alpha}(s)}{2i} &= \frac{(2\pi)^4}{2}\int d\Phi_2 F_\pi^V(s)\times T_{\pi\pi}^{\alpha *}(s,t)\\ &+ \frac{(2\pi)^4}{2}\int d\Phi_2 F_\pi^{V,\alpha}(s)\times T_{\pi\pi}^{*}(s,t)\\ &+ \frac{(2\pi)^4}{2}\int d\Phi_3 F_\pi^{V,\gamma}(s,t)\,T_{\pi\pi}^{\gamma *}(s,\{t_i\})\end{aligned}$$

Approximation: only 2π intermediate states for $F_\pi^{V,\gamma}$ and $T_{\pi\pi}^{\gamma}$:

All subamplitudes known $\Rightarrow$ $F_\pi^{V,\gamma}$ and $T_{\pi\pi}^{\gamma}$ ✓

J. Monnard, PhD thesis 2021

Evaluation of $F_\pi^{V,\alpha}$

Having evaluated all the following diagrams

J. Monnard, PhD thesis 2021

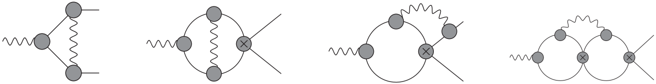

Evaluation of $F_\pi^{V,\alpha}$

Having evaluated all the following diagrams

J. Monnard, PhD thesis 2021

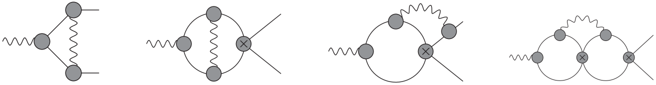

the results for $\sigma(e^+e^- \to \pi^+\pi^-(\gamma))$ look as follows:

Preliminary!

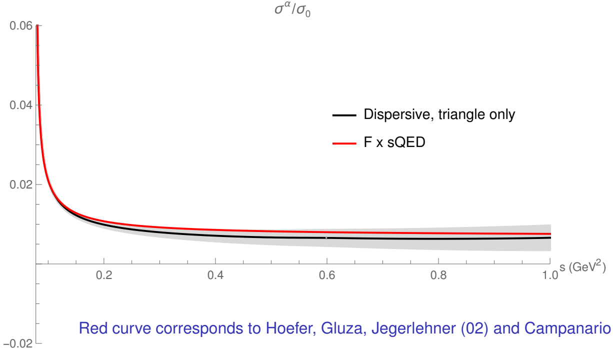

Red curve corresponds to Hoefer, Gluza, Jegerlehner (02) and Campanario et al. (19) (?)

Evaluation of $F_\pi^{V,\alpha}$

Having evaluated all the following diagrams

J. Monnard, PhD thesis 2021

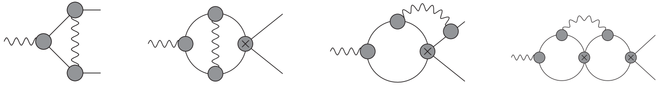

the results for $\sigma(e^+e^- \to \pi^+\pi^-(\gamma))$ look as follows:

Preliminary!

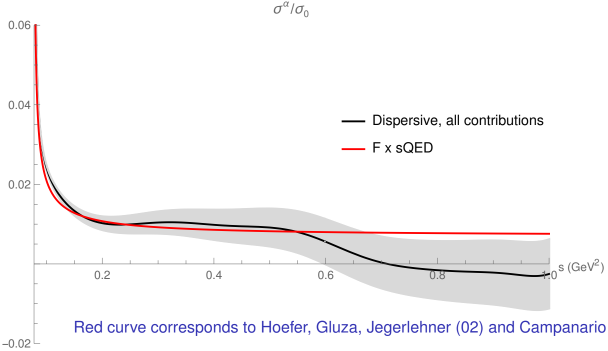

Red curve corresponds to Hoefer, Gluza, Jegerlehner (02) and Campanario et al. (19) (?)

Impact on $a_\mu^{\rm HVP}$

Ideally: use calculated RC in the data analysis (future?).

Quick estimate of the impact: thanks to M. Hoferichter and P. Stoffer

1. remove RC from the measured $\sigma(e^+e^- \to \pi^+\pi^-(\gamma))$
2. fit with the dispersive representation for $F_\pi^V(s)$
3. insert back the RC

The impact on $a_\mu^{\rm HVP}$ is evaluated by comparing to the result obtained by removing RC with $\eta(s)$ calculated in sQED

$$10^{11}\Delta a_\mu^{\rm HVP} = \begin{cases} 10.2 \pm 0.5 \pm 5 & \text{FsQED} \\ 10.5 \pm 0.5 \pm (?) & \text{triangle} \\ 13.2 \pm 0.5 & \text{full} \end{cases}$$

Outline

Introduction: $(g-2)_\mu$ in the Standard Model

Hadronic light-by-light

Hadronic Vacuum Polarization contribution
- Data-driven approach
- Lattice vs data-driven: intermediate window
- The MUonE experiment
- Radiative corrections with a dispersive approach: A_{FB} and σ

Conclusions and Outlook

Conclusions

- Data-driven evaluation of the HVP contribution (WP20): 0.6% error $\Rightarrow$ dominates the theory uncertainty
- Dominant contribution to HVP: $\pi\pi$ (<1 GeV). WP20 based on: CMD-2, SND06, BaBar, KLOE
  New puzzle: measurement by CMD-3 significantly higher!
- Recent lattice calculation [BMW(20)] has reached a similar precision but differs from the dispersive one (=from e^+e^- data).
  If confirmed $\Rightarrow$ discrepancy with experiment $\searrow$ below 2σ
- Intermediate window of BMW has been confirmed by other lattice collaborations (Aubin et al., Mainz, ETMc, RBC/UKQCD, Fermilab-HPQCD-MILC) and disagrees with data-driven [other than CMD-3, which would agree]
- Evaluation of the HLbL contribution based on the dispersive approach: 20% accuracy. Two recent lattice calculations [RBC/UKQCD(20), Mainz(21)] agree with it

Outlook

- The Fermilab experiment aims to reduce the BNL uncertainty by a factor four $\Rightarrow$ potential 7σ discrepancy
- Improvements on the SM theory/data side:
  - Situation for HVP data-driven urgently needs to be clarified:
    - Thorough scrutiny of the new CMD-3 result
    - Forthcoming measur./analyses: BaBar, Belle II, BESIII, KLOE,SND
    - Model-independent evaluation of RadCorr underway (but cannot be the culprit)
    - MuonE will provide an alternative way to measure HVP
  - HVP lattice:
    calculations with precision $\sim$ BMW for $a_\mu^{\text{HVP, LO}}$ are awaited
  - HLbL: goal of $\sim$ 10% uncertainty within reach (both data-driven and lattice)

Future: Muon $g-2$/EDM experiment @ J-PARC

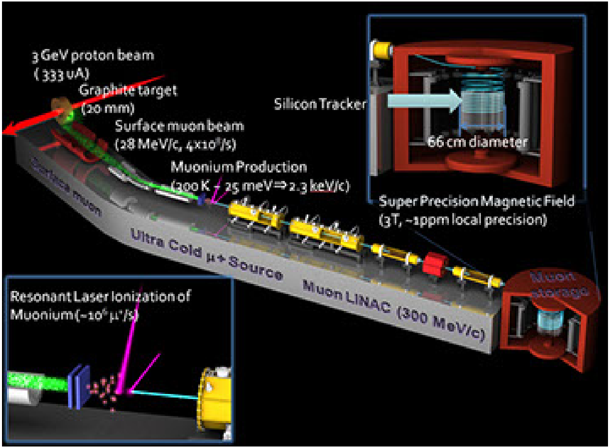

Credit: J-PARC

Backup Slides

Vector form factor of the pion

$$\langle \pi^i(p')|V_\mu^k(0)|\pi^l(p)\rangle = i\epsilon^{ikl}(p'+p)_\mu F_\pi^V(s) \qquad s=(p'-p)^2$$

Analyticity:

$$e^{-i\delta(s)}F_\pi^V(s)\in\mathbb{R} \text{ for } s+i\varepsilon,\ 4M_\pi^2\le s<\infty$$

Exact solution: Omnès (58)

$$F_\pi^V(s) = P(s)\Omega(s) = P(s)\exp\left\{\frac{s}{\pi}\int_{4M_\pi^2}^\infty \frac{ds'}{s'}\frac{\delta(s')}{s'-s}\right\} \quad ,$$

$P(s)$ a polynomial $\Leftrightarrow$ behaviour of $F_\pi^V(s)$ for $s\to\infty$ (or zeros)

- normalization fixed by gauge invariance:

$$F_\pi^V(0)=1 \qquad \overset{\text{no zeros}}{\Longrightarrow} \qquad P(s)=1$$

- $e^+e^-\to\pi^+\pi^-$ data $\Rightarrow$ free parameters in $\Omega(t)$

Free parameters

$$\Omega_1^1(s) \quad \Rightarrow \quad \begin{cases} \phi_0 = \delta_{\pi\pi}((0.8 \text{ GeV})^2) \\ \phi_1 = \delta_{\pi\pi}((1.15 \text{ GeV})^2) \end{cases}$$ [Roy eqs.]

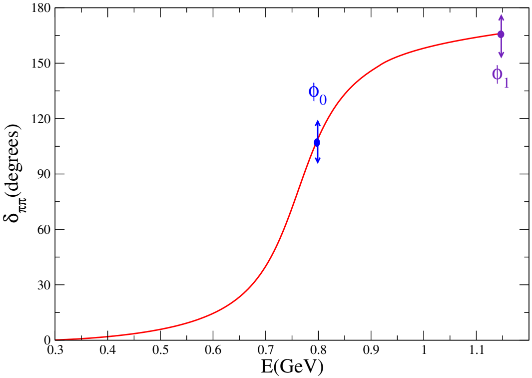

Free parameters

$$\Omega_1^1(s) \quad \Rightarrow \quad \begin{cases} \phi_0 = \delta_{\pi\pi}((0.8\ \mathrm{GeV})^2) \\ \phi_1 = \delta_{\pi\pi}((1.15\ \mathrm{GeV})^2) \end{cases} \quad \text{[Roy eqs.]}$$

$$G_\omega(s) \quad \Rightarrow \quad \begin{cases} \epsilon & \omega - \rho \text{ mixing} \\ M_\omega \end{cases}$$

Free parameters

$$\Omega_1^1(s) \Rightarrow \begin{cases} \phi_0 = \delta_{\pi\pi}((0.8\ \mathrm{GeV})^2) \\ \phi_1 = \delta_{\pi\pi}((1.15\ \mathrm{GeV})^2) \end{cases} \quad \text{[Roy eqs.]}$$

$$G_\omega(s) \Rightarrow \begin{cases} \epsilon & \omega - \rho \text{ mixing} \\ M_\omega & \end{cases}$$

$$\Omega_{\rm in}(s) \Rightarrow \begin{cases} c_2 \\ \vdots \\ c_N \end{cases} \qquad \mathrm{Im}\Omega_{\rm in}(s) = 0 \quad s \le s_{\pi\omega}$$

$$\Omega_{\rm in}(s) = 1 + \sum_{k=1}^{N} c_k (z(s)^k - z(0)^k) \qquad z = \frac{\sqrt{s_{\pi\omega} - s_1} - \sqrt{s_{\pi\omega} - s}}{\sqrt{s_{\pi\omega} - s_1} + \sqrt{s_{\pi\omega} - s}}$$